

# Electrical properties and microstructure of glass–ceramic materials from CaO–MgO–Al<sub>2</sub>O<sub>3</sub>–SiO<sub>2</sub> system

A. SACCANI, F. SANDROLINI

*Dipartimento di Chimica Applicata e Scienza dei Materiali University of Bologna, 40136 Bologna, Italy*

C. LEONELLI, T. MANFREDINI

*Dipartimento di Chimica, University of Modena, 41100 Modena, Italy*

The electrical (volume conductivity) and dielectric (loss factor and dielectric constant) properties of glass–ceramics belonging to the CaO–MgO–Al<sub>2</sub>O<sub>3</sub>–SiO<sub>2</sub> system have been studied, as a function of microstructure, in their glassy and ceramized forms on samples obtained as bulk materials or sintered powders. A possible application of these materials as substrates for electronic devices can be envisaged, on account of their low conductivities ( $<10^{-14}$  S cm<sup>-1</sup> up to 250 °C), loss factor and permittivity values.

## 1. Introduction

Glass–ceramic materials have given rise to a huge interest in material science [1–3] due to their peculiar characteristics, such as high mechanical resistance, low permittivity, electrical conductivity and the tailorability of linear expansion coefficient (high enough to match the linear expansion of others materials or extremely low to make them particularly resistant to thermal shocks). All these properties make them suitable for electronic applications as alternative substrates to the materials used nowadays (alumina, aluminium nitride, forsterite, etc.) [4–6].

In the present paper the electrical properties of a glass from the CaO–MgO–Al<sub>2</sub>O<sub>3</sub>–SiO<sub>2</sub> system, derived from materials commonly used in the ceramic glaze industry, are investigated. The aim of the paper is to verify the insulating characteristics of these materials as a function of their crystallinity, microstructure and preparation method, envisaging a possible application in electronic substrates industry. The investigated materials were prepared in the forms of sintered and bulk glassy samples and glass–ceramics henceforward obtained.

## 2. Materials and samples

The system can be simply ceramized through a suitable thermal treatment without the addition of any nucleating agent up to an extent greater than 90%, leading to a mixture of anorthite and diopside of 25 and 75 vol %, respectively. The ceramized material shows a linear expansion coefficient of  $\alpha_{35-500} = 70-80 \times 10^{-7} \text{ } ^\circ\text{C}^{-1}$  [7].

### 2.1. Bulk Samples

Glass samples (type A) were prepared as elsewhere described [7], with the following molar oxide content: 50.10 SiO<sub>2</sub>, 5.15 Al<sub>2</sub>O<sub>3</sub>, 25.03 CaO, 19.72 MgO, by pouring the melt on a hot plate and pressing them to obtain discs of about at least 25 mm in diameter and thickness up to 3 mm, bubble-free, which were subsequently polished to obtain planar surfaces. Ceramized samples (type B) were obtained from type A samples by the following heat treatment: 1 h at 900 °C, 1 h at 1000 °C and 30 min at 1100 °C, heating rate 6 °C min<sup>-1</sup>, spontaneous cooling in the kiln to avoid cracking.

### 2.2. Sintered samples

Sintered glass samples (type C) were obtained by cold pressing (up to 90 MPa) the fine powders (grain size distribution: 80% < 35  $\mu\text{m}$ , 40% < 10  $\mu\text{m}$ , 20% < 3  $\mu\text{m}$ ) obtained from type A samples by wet milling. The addition (5 wt %) of a water solution containing polyvinyl alcohol (PVA) (8 wt %) was necessary to obtain samples in the form of discs 25 mm in diameter and up to 4 mm thick. The sintered samples were obtained by heating at a temperature rate of 6 °C min<sup>-1</sup> to 900 °C, in the glass softening zone ( $T_g = 740 \text{ } ^\circ\text{C}$  [7]), and kept for 1 h at this temperature. They were then cooled spontaneously in the kiln. Previous differential thermal analysis (DTA) and X-ray analyses showed that no devitrification processes take place up to this temperature [8].

Ceramized (type D) were obtained from type C samples by heating up to 1100 °C at 6 °C min<sup>-1</sup>, kept at this temperature for 1 h, and subsequently cooled

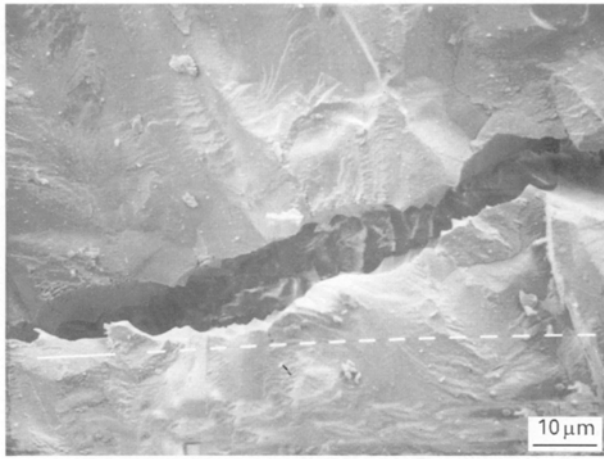


Figure 1 Microstructure of the fractured surface of sample B.

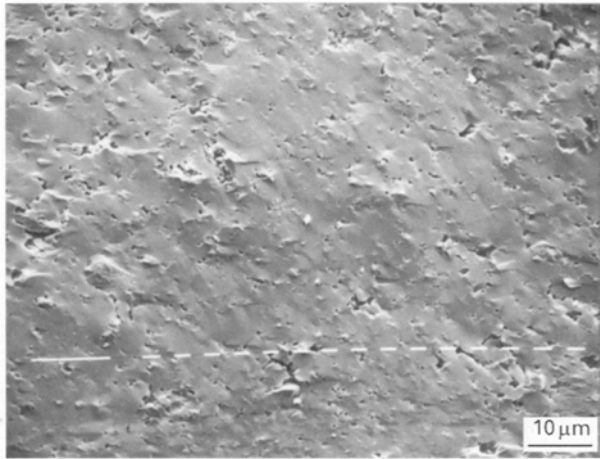


Figure 2 Microstructure of the fractured surface of sample C.

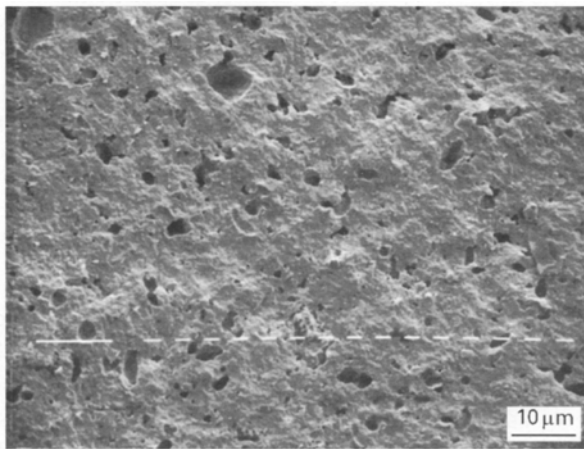


Figure 3 Microstructure of the fractured surface of sample D.

spontaneously at room temperature. The discs were then coated with either gold or graphite by evaporation under vacuum, with a suitable three-terminal electrode configuration.

### 3. Experimental procedure

All electrical and dielectric measurements were performed in dynamic vacuum. The volt-ampereometric method was used to determine the volume electrical

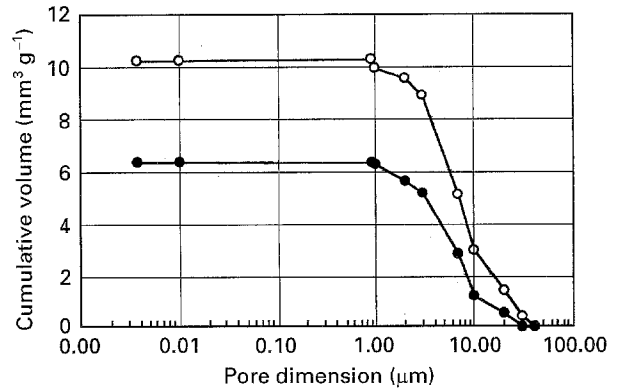


Figure 4 Cumulative intruded volume for investigated samples C (●) and (○) D as a function of pore size.

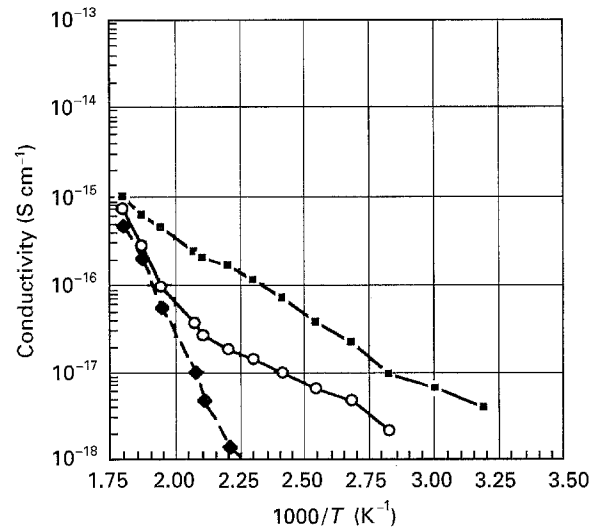


Figure 5 Electrical conductivity of sample A at 1 (■), 10 (○), 60 (◆) min after the voltage application, as a function of temperature.

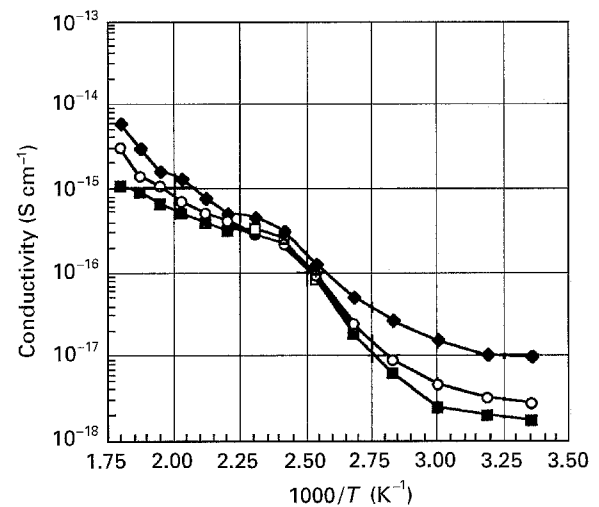


Figure 6 Electrical conductivity sample B at 1 (◆), 10 (○), 60 (■) min after the voltage application, as a function of temperature.

conductivity by means of a three terminal cell, described elsewhere [9], as preliminary tests had underlined the insulating character of these glasses [10]. An electric field of 5 kV cm<sup>-1</sup> for all samples was applied. Dielectric measurements were carried out as a function of temperature in the frequency range 10<sup>-2</sup>–10<sup>6</sup> Hz, from room temperature up to 250 °C, with

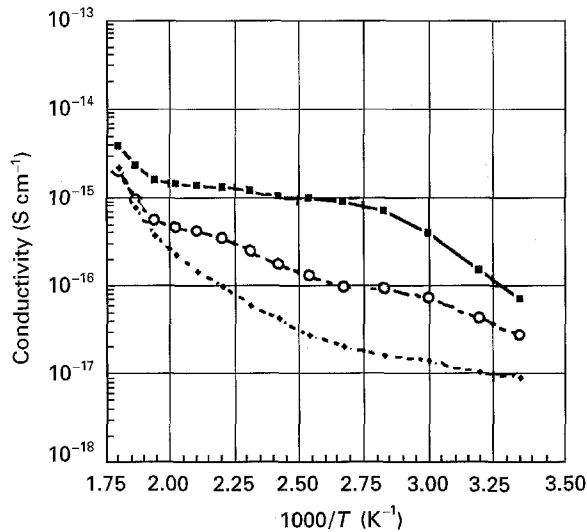


Figure 7 Electrical conductivity of sample C at 1 (■), 10 (○), 60 (◆) min after the voltage application.

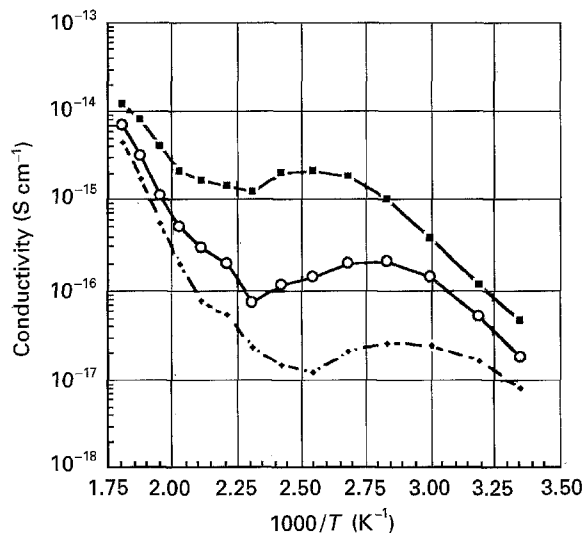


Figure 8 Electrical conductivity of sample D at 1 (■), 10 (○), 60 (◆) min after the voltage application, as a function of temperature.

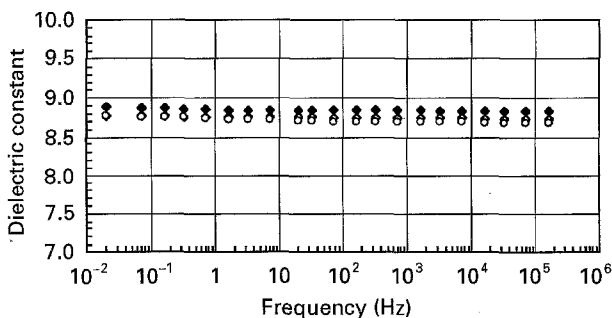


Figure 9 Dielectric constant of sample A at 250 (◆), 100 (◇), 25(○)°C as a function of frequency.

instrumentation described elsewhere [11, 12]. Hamon treatment of discharging currents allowed to obtain loss factor in the ultralow frequency range ( $10^{-5}$ – $10^{-2}$  Hz).

Microporosity was evaluated by means of a Carlo Erba 2000 mercury porosimeter, equipped with macropore unit, in the range 0.0037–360  $\mu\text{m}$ . Microstructures of undisturbed fractured surfaces were observed

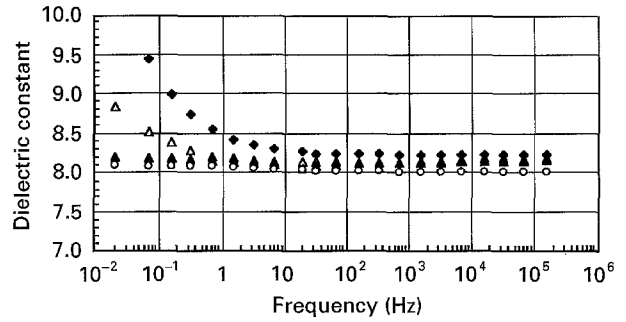


Figure 10 Dielectric constant of B sample at 250 (◆), 200 (△), 150 (▲), 25(○)°C as a function of frequency.

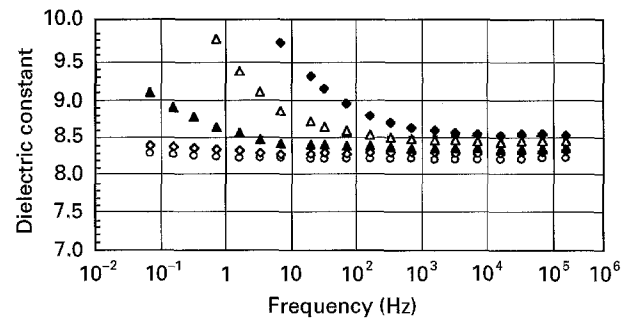


Figure 11 Dielectric constant of sample C at 250 (◆), 200 (△), 150 (▲), 100 (◇), 25 (○)°C as a function of frequency.

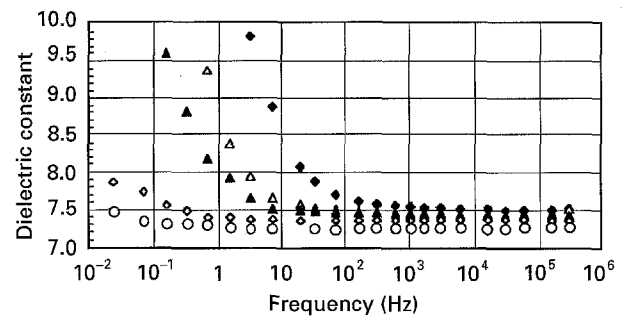


Figure 12 Dielectric constant of sample D at 250 (◆), 200 (△), 150 (▲), 100 (◇), 25(○)°C as a function of frequency.

by scanning electron microscope (SEM; Philips 501 B) after gold evaporation under vacuum.

#### 4. Results and discussion

Fig. 1 depicts the fracture surface of B samples: crystals grow perpendicularly to the sample surface [7], creating an almost poreless microstructure but leaving some large crevices in the centre. Figs 2 and 3 depict the microstructure of C and D samples, respectively: both samples appear well sintered and exhibit limited porosity approaching a spherical shape.

In Fig. 4, mercury porosimetry data are shown for C and D samples. Sample D shows, on account of the volume reduction effect caused by ceramization, an overall porosity higher than that of sample C, with a larger average pore size.

Figs 5–8 show volume electrical conductivity of A, B, C and D samples as a function of temperature at different times after voltage application, in the same temperature range (25–260 °C). All samples behave as

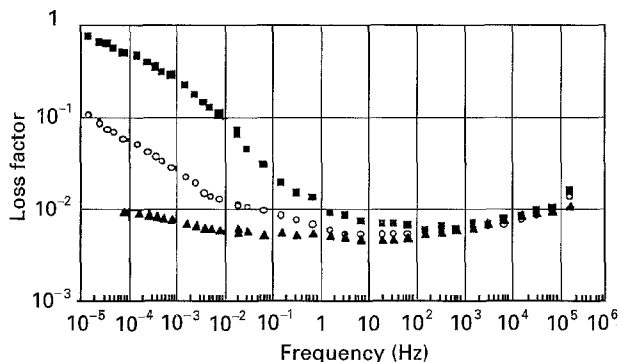


Figure 13 Loss factor of sample A as a function of frequency at constant temperature: ( $\blacktriangle$ ) 25, ( $\circ$ ) 100, ( $\blacksquare$ ) 250°C.

insulators, even at the highest temperatures, showing wide conductivity transients as a function of time, particularly at the lowest temperatures. Measurements carried out with different types of electrodes (Au, C, Ag) did not reveal meaningful changes in conductivity. The devitrification process does not induce remarkable changes in conductivity values as found for other glass ceramic materials [13–15], which, how-

ever, exhibited higher conductivity in the same temperature range. The apparent activation energy for conduction evaluated for samples A and D at high temperatures ( $>180^\circ\text{C}$ ) and 60 min voltage application, where nearly steady values of conductivity were attained, is 1.19 eV. Moreover, a slight increase in conductivity is found in the samples obtained from powders compared to the bulk ones, probably on account of the unavoidable presence of impurities (ions) coming from either the milling process or from the binder decomposition. The electrical behaviour of all materials, particularly the independence of conductivity on electrode composition, hints at an ionic mechanism of conduction. Relaxation phenomena are present in ceramized samples: while there is a very slight dependence on charging time in B samples, peak positions shift to lower temperatures as charging time increases in samples D. These processes can be related to charge carrier accumulation at grain boundaries between different phases, i.e. to Maxwell–Wagner–Sillars (MWS) relaxation type.

Figs 9–12 show dielectric constant,  $\epsilon'$ , for A, B, C, and D samples, respectively, as a function of frequency

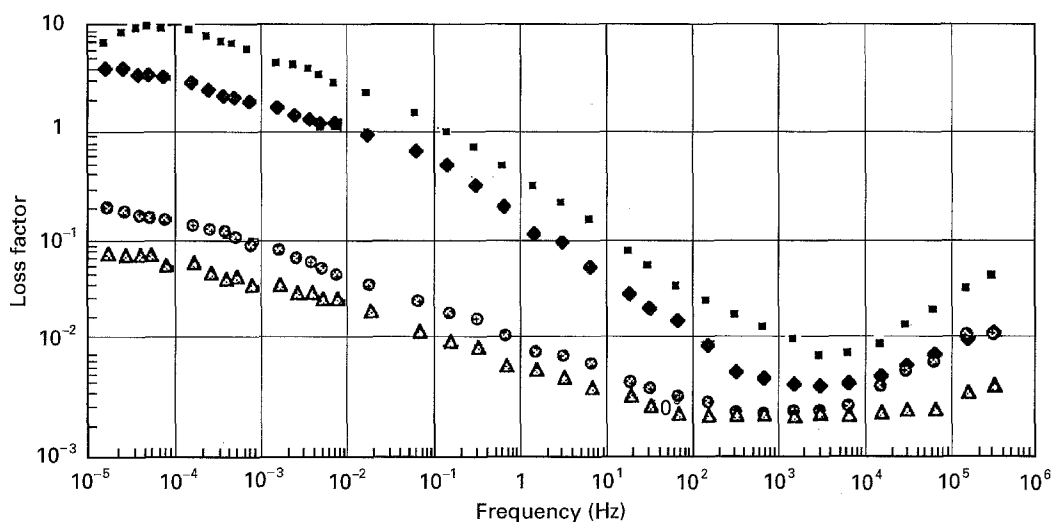


Figure 14 Loss factor of sample B as a function of frequency at constant temperature: ( $\triangle$ ) 25, ( $\circ$ ) 100, ( $\blacklozenge$ ) 200, ( $\blacksquare$ ) 250°C.

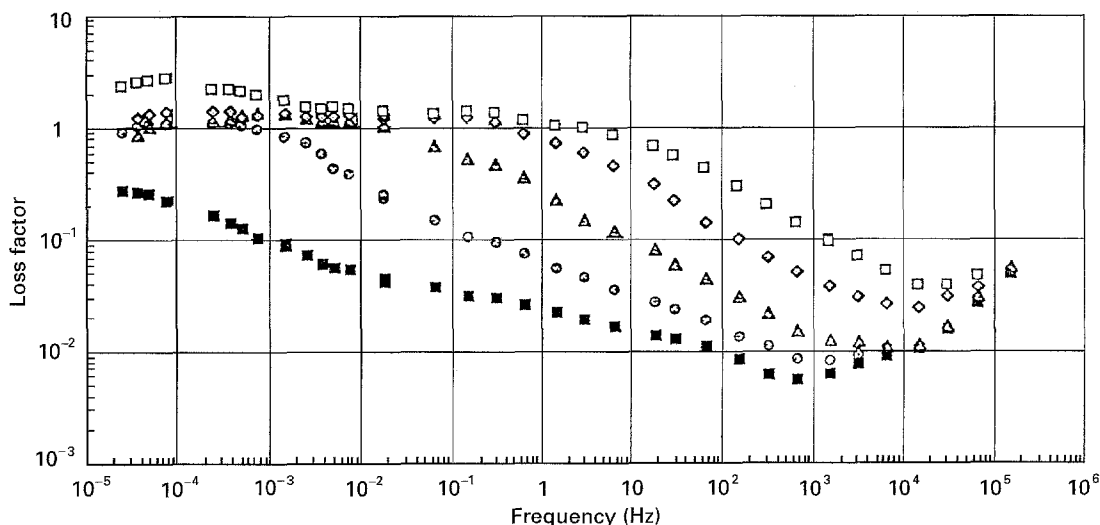


Figure 15 Loss factor of sample C as a function of frequency at constant temperature: ( $\blacksquare$ ) 25, ( $\circ$ ) 100, ( $\triangle$ ) 150, ( $\diamond$ ) 200, ( $\square$ ) 250°C.

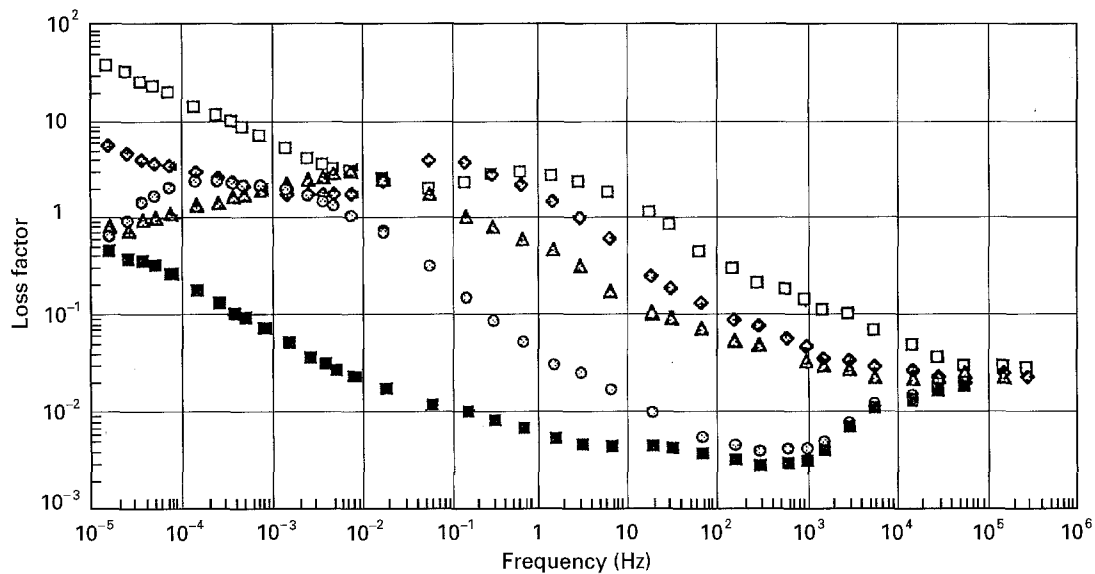


Figure 16 Loss factor of sample D as a function of frequency at constant temperature: (■) 25, (○) 100, (△) 150, (◇) 200, (□) 250 °C.

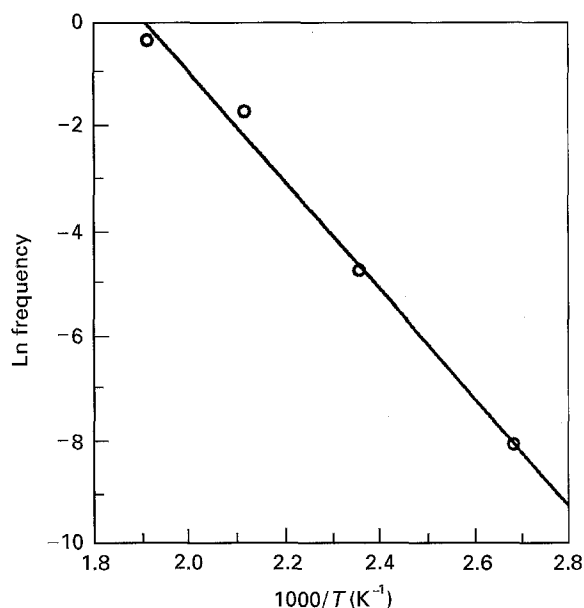


Figure 17 Transition map for relaxation phenomenon in the ceramized sample D.

in the temperature range from 25 to 250 °C. Values are almost independent of frequency at low temperatures (<100 °C), but tend to increase below 10<sup>2</sup> Hz, particularly on sintered samples. Permittivity decreases in ceramized samples, on account of the higher order of the material, and in sintered ones, on account of their higher porosity.

Figs 13–16 depict loss factor,  $\epsilon''$ , of A, B, C and D samples, respectively, as a function of frequency in the same temperature range. The most remarkable feature is the presence of a relaxation process in sample D at relatively low frequencies, whose activation energy calculated from Fig. 17, is about 1.1 eV, a value which is relatively close to that found for d.c. conductivity. The origin of the process should thus be related to charge carrier motion, and it should thus be recognized as a conduction relaxation loss, analogous to that found in d.c. measurements. The process, in

a less clear way, is present also in sample C, probably indicating the appearance of more ordered domains, which, however, could not be distinguished by X-ray analysis.

Loss factor tends to increase in all samples as frequency lowers, witnessing the presence of ions (impurities), which is higher in samples C and D, as mentioned previously.

## 5. Conclusions

1. The investigated materials show, in all their forms, an insulating behaviour ( $\sigma < 10^{-14} \text{ S cm}^{-1}$ ) up to 250 °C; they also show low loss factor values, which tend to increase in the ultra-low frequency range (<10<sup>-2</sup> Hz) at temperature higher than 100 °C, a phenomenon which must be ascribed to the presence of impurity ions in the materials;
2. The dielectric constant of the materials is lower than that of alumina: the ceramization process induces a decrease in values on account of the increased structural order.
3. A relaxation process appears in the sample ceramized from powders both in d.c. and in a.c., at low frequency: the energy of activation of the a.c. process and that of conductivity are closer. Both phenomena should thus have the same origin, i.e. the charge carrier accumulation at either grain boundaries between different crystalline phases or the residual glassy zones, and can be classified as MWS relaxations.
4. The overall electrical behaviour of materials is comparable to that of the most applied, but more expensive, substrate materials in electronic industry, and is therefore consistent with their possible employment in this field.

## Acknowledgements

Support from "Progetto Finalizzato Materiali Speciali per Tecnologie Avanzate" of CNR is gratefully acknowledged.

## References

1. P. W. McMILLIAN, "Glass-ceramics" (Academic Press, London, 1979).
2. Z. STRAND, "Glass-ceramic materials" (Elsevier, New York, 1986).
3. M. H. LEWIS, "Glasses and glass-ceramics" (Chapman & Hall, London, 1989) Ch. 7.
4. G. PARTRIDGE, C. A. ELYARD and M. BUDD, in "Glass-ceramics in substrate application", edited by M. H. Lewis (Chapman & Hall, London, 1989).
5. G. PARTRIDGE, *Adv. Mater.* **3** (1990) 147.
6. I. O. OWATE and R. FREER, *J. Mater. Sci.* **25** (1990) 5291.
7. C. LEONELLI, T. MANFREDINI, M. PAGANELLI and G. C. PELLACANI, *ibid.* **26** (1991) 5041.
8. L. BARBIERI, C. LEONELLI, T. MANFREDINI, M. PAGANELLI, G. C. PELLACANI, *J. Therm. Anal.* **38** (1992) 2639.
9. F. SANDROLINI, *J. Phys. E: Sci. Instr.* **13** (1980) 152.
10. F. SANDROLINI, A. SACCANI, L. BARBIERI, C. LEONELLI, T. MANFREDINI and G. C. PELLACANI, in Proceedings of the Congress "Omaggio Scientifico a Renato Turriziani", Roma, 23-24 April 1992, vol. II, p. 409.
11. G. MARRONE, A. MOTORI, P. NICOLINI and F. SANDROLINI, in Proceedings of CIGRE, September 1992, Paper 15-402, Paris.
12. F. SANDROLINI and P. CREMONINI, *Materie Plastiche ed Elastomeri*, **7-8** (1979) 405.
13. H. HOSONO and Y. ABE, *Solid State Ionics* **44** (1991) 293.
14. T. MINAMI, Y. TAKUMA and M. TANAKA, *J. Electrochem. Soc.* **124** (1977) 1659.
15. Z. PEINAN, *B. Y. Tangci*, **17** (1989) 1.

*Received 3 January  
and accepted 13 June 1996*